Laser cavity with Van der Pol dynamics

M. Lozano
Depto. de Actuaría, Física y Matemáticas,
Universidad de las Américas Puebla, Puebla, México 72810.
e-mail: mara.lozanomz@udlap.mx

A. Kir'yanov
Centro de Investigaciones en Óptica A.C.,
Loma del Bosque 115 Col. Campestre, 37150 León Gto., México.
e-mail: alejandrokir@gmail.com

A. Pisarchik
Center for Biomedical Technology, Technical University of Madrid,
Campus Montegancedo, 28223 Pozuelo de Alarcon, Madrid, Spain.
e-mail: alexander.pisarchik@ctb.upm.es

V. Aboites*
Centro de Investigaciones en Óptica,
Loma del Bosque 115, Col. Campestre, 37150 León Gto., México.
e-mail: aboites@cio.mx

Received 21 September 2020; accepted 21 October 2020

In this article, a beam within a ring phase conjugated laser is described by means of a Van der Pol bidimensional dynamic map using an ABCD matrix approach. Explicit expressions for the intracavity chaos-generating matrix elements were obtained; furthermore, computer calculations for different values of Van der Pol map's parameters were made. The rich-dynamic behavior displays periodicity when the parameter μ (which determines the non-linearity term) takes values around zero. These results were observed in phase diagrams and diagrams of the optical thickness of the intracavity element.

Keywords: Van der Pol map; phase conjugate; laser dynamics.

PACS: 42.60.Da; 05.45.Gg; 05.45.Pq

DOI: https://doi.org/10.31349/RevMexFis.67.154

1. Introduction

Balthazar Van der Pol (1899-1959) was a Dutch electrical engineer. During the 1920s and 1930s, he worked towards the development of radio and vacuum tube technology. Accordingly, he developed an interesting mathematical model, now known as the Van der Pol equation, to describe stable oscillations, called limit cycles, in electrical circuits that employ vacuum tubes. When these circuits are driven near the limit cycle, they become entrained, *i.e.*, the driving signal pulls the current along with it. Van der Pol and his colleague, Van der Mark, reported that at certain drive frequencies, an irregular noise was heard, which was later found to be the result of deterministic chaos [1]. Recently, Van der Pol equation has been used in both physical and biological sciences, among many other areas. For instance, Fitzhugh [2] and Nagumo [3] used the equation on a planar field to model the action potential of neurons. The equation was also employed in seismology to model the plates in a geological fault [4]. Also, Shuto [5] has used this equation to study cavity formation modeling of fiber fuse in single-mode optical fibers.

An important research area for nonlinear optics is optical phase conjugation (OPC). One possible way to obtain OPC is through Four-Wave Mixing (FWM), where a link is established between two coherent optical beams propagating in opposite directions with reversed wavefronts and identical transverse amplitude distributions [6]. In addition to FWM, there are many further approaches to produce the backward PC beam; another approach is based on a variety of backward stimulated scattering processes such as Brillouin (SBS), Raman (SRS) or Kerr [7,8,9], of which the last one is based on one-photon or multi-photon pumped backward stimulated emission-processes. The basic characteristic of a pair of PC beams is that the aberration influence imposed on the forward beam propagating through an inhomogeneous or disturbing medium can be automatically removed for the backward beam passing through the same medium.

In the present work, the dynamical behavior of a beam that spatially behaves according to a Van der Pol map, here called a Van der Pol beam, within a ring phase-conjugated cavity is modeled. As shown, the behavior of a beam may be obtained by making an arbitrary well-defined chaotic map [10,11,12]. Particularly, the Henón [14], Bogdanov [15], Ikeda [16], Duffing [17,18], Standard [19] and Tinkerbell maps [20, 21] were employed, among others. Here, for the first time to the best of our knowledge, a PC laser ring cavity

is designed to produce Van del Pol beams within certain well-defined parameters. The structure of this article is as follows. In Sec. 2, a derivation of the Van der Pol map is sketched following Refs. [22,23,24]. In Sec. 3, the ABCD matrix formalism is used to describe an optical cavity; as known, this formalism is commonly used in paraxial optics [25], allowing the representation of each optical component as a 2×2 matrix. Furthermore, the two-dimensional map converted into a theoretical matrix system enables us to reproduce a complex dynamical behavior of the Van der Pol map within a PC ring cavity. As follows, in Subsecs. 3.1 and 3.2, a general case of the Van der Pol beams is approximately obtained. In Sec. 4, the numerically obtained results are discussed. Finally, in Sec. 5, our main conclusions are given.

2. Van der Pol map

There is a large list of bi-dimensional maps (see [26], for example), and one of them is the Van der Pol map. It is known that many oscillating circuits can be modeled by a second-order differential equation of the form

$$\frac{d^2x}{dt^2} + f(x)\frac{dx}{dt} + g(x) = 0. \tag{1}$$

This differential equation is known as Lienard's equation [27]. Clearly, it may be interpreted as the equation of motion for a unit mass object subject to a nonlinear damping force and a nonlinear restoring force. Lienard's equation may also be written in the phase plane as

$$\begin{cases} \dot{x} = y \\ \dot{y} = -g(x) - f(x)y \end{cases}, \tag{2}$$

where under appropriate $f(x)$ and $g(x)$, the system has a unique, stable limit cycle [23,28,29]. This is explained in the following theorem.

Theorem 2.1 *(Lienard's theorem). Suppose that $f(x)$ and $g(x)$ satisfy the following conditions:*

1. *$f(x)$ and $g(x)$ are continuously differentiable $\forall x$.*
2. *$g(x)$ is an odd function* (*or $g(-x) = -g(x)$*).
3. *$g(x) > 0$ for $x > 0$.*
4. *$f(x)$ is an even function* (or $f(-x) = f(x)$).
5. The odd function $F(x) = \int_0^x f(u)du$ *has exactly one zero at $x = a$, is negative and non-decreasing for $x > a$* and $\lim_{x\to\infty} F(x) = \infty$.

Then, the system (2.2) has a unique, stable limit cycle surrounding the origin at the phase plane.

The Van der Pol oscillator is a model that was originally developed to describe the behavior of nonlinear vacuum tube circuits. In a self-maintained electrical RLC circuit, where the capacitor C is initially charged, and R is a non-linear resistance, the tension is defined as [25]

$$U_L + U_R + U_C = 0, \tag{3}$$

where

$$U_L = L\frac{di}{d\tau}, \tag{4}$$

$$U_R = -R_0 i_0 \left(\frac{i}{i_0} - \frac{1}{3}\left[\frac{i}{i_0}\right]^3\right), \tag{5}$$

and

$$U_c = \frac{1}{c}\int i d\tau, \tag{6}$$

with i_0 and R_0 being the current and normalized resistance, respectively. Substituting Eqs. (4), (5) and (6) in (3), we have

$$L\frac{di}{d\tau} - R - 0i_0\left(\frac{i}{i_0} - \frac{1}{3}\left[\frac{i}{i_0}\right]^3\right) + \frac{1}{c}\int i d\tau = 0. \tag{7}$$

Differentiating Eq. (7) with respect to τ,

$$L\frac{d^2i}{d\tau^2} - R_0\left(1 - \frac{i^2}{i_0^2}\right)\frac{di}{d\tau} + \frac{i}{c} = 0, \tag{8}$$

introducing

$$x = \frac{i}{i_0}, \tag{9}$$

and

$$t = \omega_e \tau, \tag{10}$$

where $\omega_e = 1/\sqrt{LC}$, we obtain

$$\frac{d}{d\tau} = \omega_e \frac{d}{dt}, \tag{11}$$

and

$$\frac{d^2}{d\tau^2} = \omega_e^2 \frac{d^2}{dt^2}. \tag{12}$$

By substituting Eqs. (11) and (12) in Eq. (8) yields

$$\frac{d^2x}{dt^2} - R_0\sqrt{\frac{C}{L}}(1 - x^2)\frac{dx}{dt} + x = 0. \tag{13}$$

By setting $\mu = R_0\sqrt{C/L}$, Eq. (13) can be transformed to the following form:

$$\frac{d^2x}{dt^2} - \mu(1 - x^2)\frac{dx}{dt} + x = 0. \tag{14}$$

Since this differential equation is isomorphic to Lienard's Eq. (1), it satisfies Eq. (1). In this sense, the Van der Pol equation obeys Lienard's transformation:

$$\dot{x} = y \tag{15}$$

and

$$\dot{y} = \mu(1 - x^2)y - x. \tag{16}$$

There are many methods to numerically solve non-linear differential equations, such as the Runge-Kutta or Euler discretization methods. Using the last one, we rewrite the above system as [30]

$$y_{n+1} = y_n + h\theta - n, \tag{17}$$

and

$$\theta_{n+1} = \theta_n + h(\mu[1 - y_n^2]\theta_n - y_n), \tag{18}$$

where y_n and θ_n are the scalar variables, h is a discretization step, and μ is the map parameter. This system may be written in the matrix form of a Van der Pol map as

$$\begin{pmatrix} y_{n+1} \\ \theta_{n+1} \end{pmatrix} = \begin{pmatrix} A & B \\ C & D \end{pmatrix} \begin{pmatrix} y_n \\ \theta_n \end{pmatrix}, \tag{19}$$

with elements

$$A = 1, \tag{20a}$$

$$B = h, \tag{20b}$$

$$C = -h, \tag{20c}$$

and

$$D(h, \mu, y_n) = 1 + h\mu(1 - y_n^2). \tag{20d}$$

3. ABCD optic matrix of the Van der Pol map in a ring PC cavity

It is known that an optical system may be described by a 2×2 matrix in the paraxial optics approximation. Assuming cylindrical symmetry around the optical axis and defining a z optical axis, both the perpendicular distance of any ray to the optical axis and its angle to the same axis are given by $y(z)$ and $\theta(z)$ when the ray undergoes a transformation as it travels through an optical system represented by the matrix $[A, B, C, D]$; the resultant values of y and θ are given by

$$\begin{pmatrix} y_{n+1} \\ \theta_{n+1} \end{pmatrix} = \begin{pmatrix} A & B \\ C & D \end{pmatrix} \begin{pmatrix} y_n \\ \theta_n \end{pmatrix}, \tag{21}$$

For an optical system, it is possible to obtain the total transformation matrix through the product of all the matrices that describe the elements of the optical system. In the considered ring cavity shown in Fig. 1, there are two plane mirrors [M] and an ideal PC mirror [PM], separated by a distance d. The matrices which represent these two elements are: identity matrix

$$\begin{pmatrix} 1 & 0 \\ 0 & 1 \end{pmatrix}$$

for mirrors $[M]$,

$$\begin{pmatrix} 1 & 0 \\ 0 & -1 \end{pmatrix}$$

for the ideal PC mirror $[M]$,

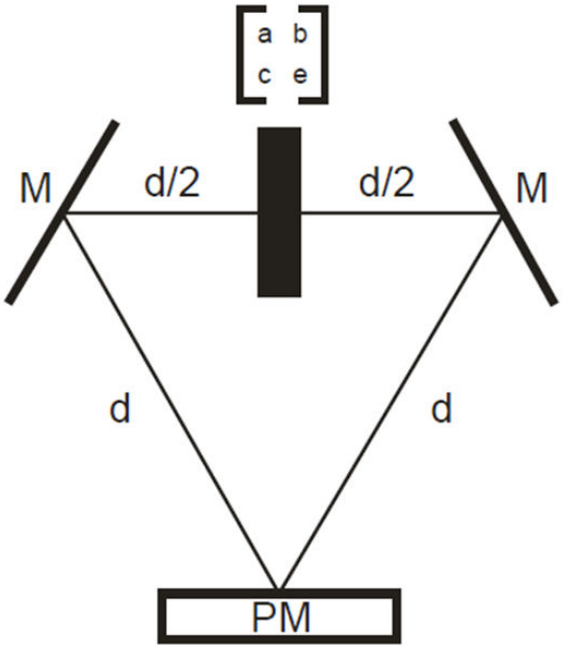

FIGURE 1. Schematic diagram of the phase conjugated ring resonator studied. There are two plane mirrors [M] and an ideal Phase Conjugated Mirror [PM], separated by a distance d, and chaos generating device represented by matrix $[a, b, c, e]$.

$$\begin{pmatrix} 1 & d \\ 0 & 1 \end{pmatrix}$$

for the propagation through distance d, and

$$\begin{pmatrix} a & b \\ c & d \end{pmatrix}$$

for the chaos generating device that is located between the two plane mirrors $[M]$ at a distance $d/2$.

For this system, the total transformation matrix $[A, B, C, D]$ for a completed round trip is:

$$\begin{aligned} \begin{pmatrix} A & B \\ C & D \end{pmatrix} = &\begin{pmatrix} 1 & 0 \\ 0 & -1 \end{pmatrix} \begin{pmatrix} 1 & d \\ 0 & 1 \end{pmatrix} \begin{pmatrix} 1 & 0 \\ 0 & 1 \end{pmatrix} \\ &\times \begin{pmatrix} 1 & d/2 \\ 0 & 1 \end{pmatrix} \begin{pmatrix} a & b \\ c & d \end{pmatrix} \begin{pmatrix} 1 & d/2 \\ 0 & 1 \end{pmatrix} \\ &\times \begin{pmatrix} 1 & 0 \\ 0 & 1 \end{pmatrix} \begin{pmatrix} 1 & d \\ 0 & 1 \end{pmatrix}; \end{aligned} \tag{22}$$

The above one round trip total transformation matrix is:

$$\begin{pmatrix} a + (3/2)cd & b + (3/2)d(2a + 3cd - 2e) \\ -c & -(3/2)cd - e \end{pmatrix} \tag{23}$$

As seen in the matrix in Eq. (23), each of the elements depends on the elements of the map generating matrix device $[a, b, c, e]$. However, if one does want a specific map to describe a beam within an optical cavity, then each trip of the beam described by (y_n, θ_n) ought to be an iteration of the map. Then, the matrix $[A, B, C, D]$ of the map Eq. (19) must be equated to the cavity matrix in Eq. (23), in order to generate a dynamic map for (y_n, θ_n) in accordance with the Van der Pol map.

Notice that result Eq. (23) is only valid for a small b, *i.e.*, $b \approx 0$. This is because before and after the chaos generating element $[a, b, c, e]$, we have a propagation distance of $d/2$. For a general case, we have:

$$\begin{pmatrix} A & B \\ C & D \end{pmatrix} = \begin{pmatrix} 1 & 0 \\ 0 & -1 \end{pmatrix} \begin{pmatrix} 1 & d \\ 0 & 1 \end{pmatrix} \begin{pmatrix} 1 & 0 \\ 0 & 1 \end{pmatrix} \begin{pmatrix} 1 & (d-b)/2 \\ 0 & 1 \end{pmatrix} \begin{pmatrix} a & b \\ c & d \end{pmatrix} \begin{pmatrix} 1 & (d-b)/2 \\ 0 & 1 \end{pmatrix} \times \begin{pmatrix} 1 & 0 \\ 0 & 1 \end{pmatrix} \begin{pmatrix} 1 & d \\ 0 & 1 \end{pmatrix}; \tag{24}$$

Then, the complete round trip transformation matrix in the general case is

$$\begin{pmatrix} a + (c/2)(b - 3d) & (1/4)(b^2c - 2b[-2 + a + 3cd - e] + 3d[2a + 3cd + 2e]) \\ -c & (1/2)(bc - 3cd - 2e) \end{pmatrix} \tag{25}$$

Thus, matrix (23) describes a simplified ideal case, whereas matrix (25) describes a general case, more complex and realistic.

3.1. Van der Pol beams

Matrix (23) describes a round trip total transformation. Each round trip within the cavity is determined by the iteration parameters (y_n, θ_n), providing the dynamics of the system. In order to have a system that exhibits Van der Pol behavior, and therefore, that of Van der Pol beams, the $[A, B, C, D]$ matrix (19) must be equated to (23). Hence,

$$a + \frac{3}{2}cd = 1, \tag{26a}$$

$$\frac{3}{2}ad + b + \frac{9}{4}cd^2 + \frac{3}{2}ed = h, \tag{26b}$$

$$c = h, \tag{26c}$$

and

$$-\frac{3}{2}cd - e = 1 + h\mu(1 - y_n^2). \tag{26d}$$

These equations define a system with variables a, b, c, e, which guarantee the behavior of a beam (y_n, θ_n), governed by Van der Pol map. Obtaining solutions, these elements may be written in terms of the map's parameters μ and h, and of variables y_n and θ_n, as:

$$a = \frac{1}{2}(2 - 3dh), \tag{27a}$$

$$b = \frac{1}{4}(4h + 9d^2h + 6dh\mu - 6dhy_n^2\mu), \tag{27b}$$

$$c = h, \tag{27c}$$

and

$$e = \frac{1}{2}(-2 - 3dh - 2h\mu + 2hy_n^2\mu). \tag{27d}$$

3.2. Van der Pol beams: general case

As mentioned before, a particular case is when the optical length of the chaos generator device is negligible (approximately zero). In the general case, b can take any value within the limitations of the parameter d, *i.e.*, $b < d$.

Both matrices (19) and (25) must be equated, giving rise to the following system of equations:

$$a - \frac{c}{2}(b - 3d) = 1, \tag{28a}$$

$$\frac{1}{4}(b^2c - 2b[-2 + a + 3cd - e] + 3d[2a + 3cd + 2e]) = h, \tag{28b}$$

$$c = h, \tag{28c}$$

The solution of this system is as follows:

$$a = \frac{1}{4}(8 + 2h\mu - 2hy_n^2 + P), \tag{29a}$$

$$b = \frac{4 + 6dh + 2h\mu - 2hy_n^2\mu + P}{2h}, \tag{29b}$$

$$c = h, \tag{29c}$$

and

$$d = \frac{1}{2}(-h\mu + hy_n^2\mu + Q), \tag{29d}$$

where

$$P = \sqrt{(-4 - 6dh - 2h\mu + 2hy_n^2\mu)^2 - 4h(4h + 9d^2h + 6dh\mu - 6dhy_n^2\mu)}. \tag{30}$$

and

$$Q = \sqrt{4 + 12dh - 4h^2 + 4h\mu - 4hy_n^2\mu + h^2\mu^2 - 2h^2y_n^2\mu^2 + h^2y_n^4\mu^2}. \tag{31}$$

4. Numerical experiment

The dynamic behavior of the PC cavity in phase space was studied through numerical iteration of the obtained matrices describing the system. In order to find valid trajectories, there are considerations that have to be taken into account. The phase plane values for y_n and θ_n must be real numbers at every iteration; diverging trajectories are only mathematical possibilities, since they cannot be related to any physical sense. Also, the b_n intracavity element from the matrices must be greater than zero and smaller than the mirror separation distance d in the cavity at every iteration. These conditions ensure that the trajectories are on the real phase plane and within a stable trajectory, given that the b_n element is related to the total distance traveled by the Van der Pol beam within the cavity.

The iterations were carried out for different values of μ and h. As it was stated, μ represents a non-linearity term of the Van der Pol map; we will explore values for this parameter around zero. The stability and chaos of the Van der Pol map in terms of the parameter μ and step h are presented in

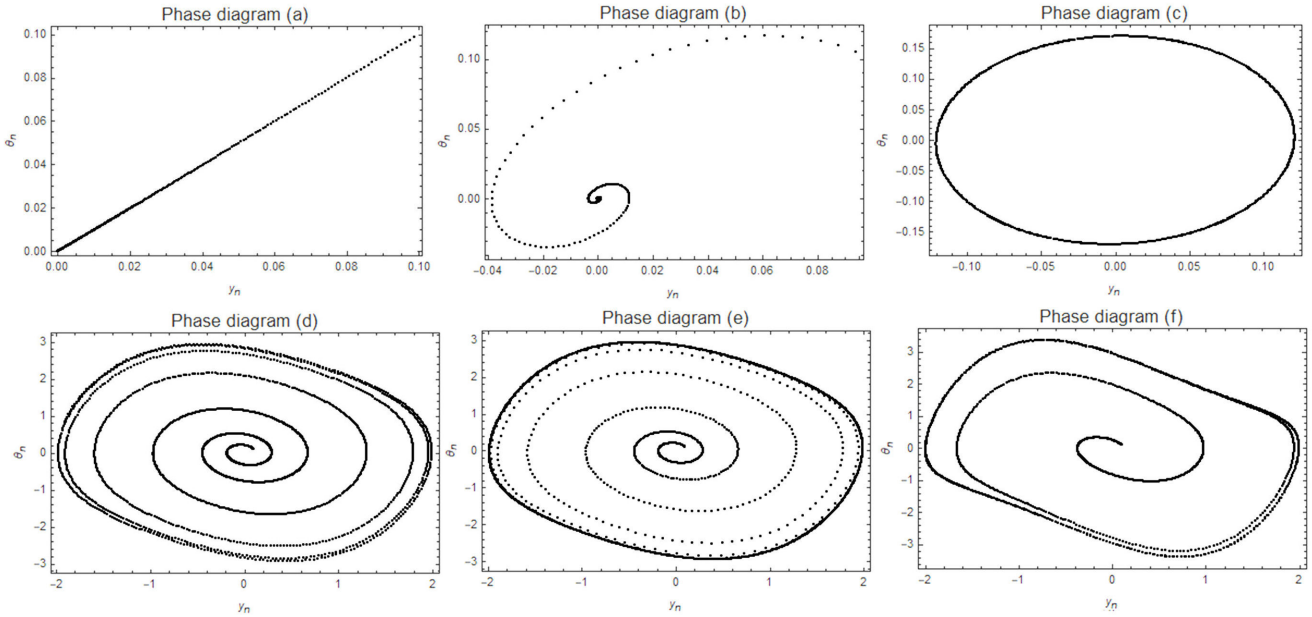

FIGURE 2. Phase space (y_n, θ_n) trajectories for parameters a) $\mu = -1.5$ $h = 0.0250$, b) $\mu = -0.5$ $h = 0.1196$, c) $\mu = 0$ $h = 0.0923$, d) $\mu = 0.2$ $h = 0.0282$, e) $\mu = 0.2$ $h = 0.0846$, f) $\mu = 0.5$ $h = 0.0250$. In all cases $d = 1$.

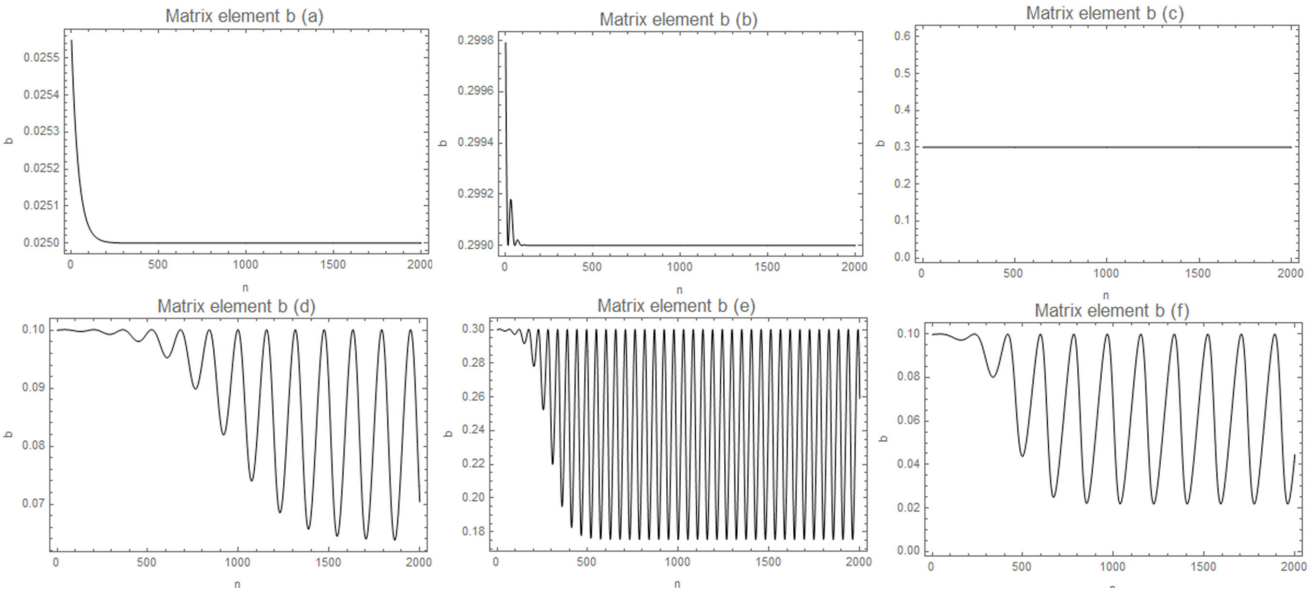

FIGURE 3. Time series of intracavity element b_n for 2000 iterations for parameters a) $\mu = -1.5$ $h = 0.0250$, b) $\mu = -0.5$ $h = 0.1196$, c) $\mu = 0$ $h = 0.0923$, d) $\mu = 0.2$ $h = 0.0282$, e) $\mu = 0.2$ $h = 0.0846$, f) $\mu = 0.5$ $h = 0.0250$. In all cases $d = 1$.

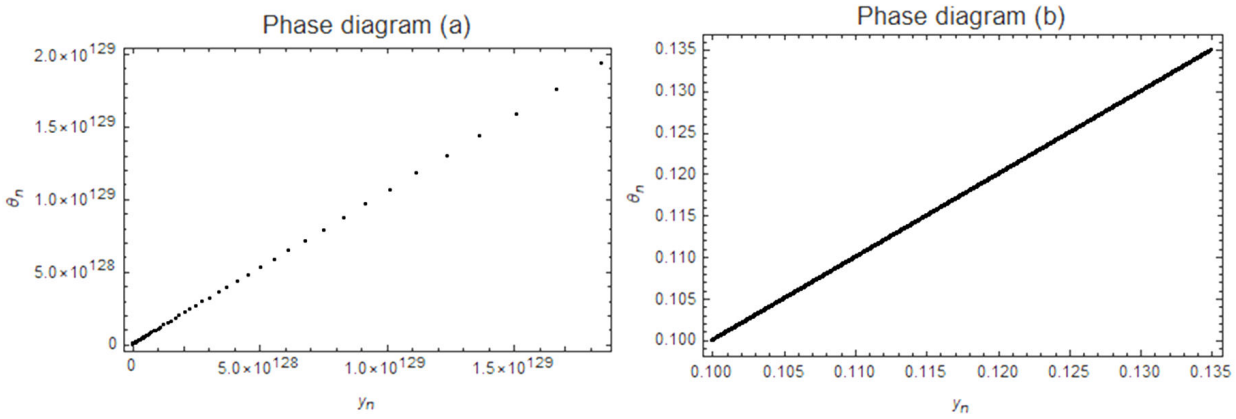

FIGURE 4. Phase space (y_n, θ_n) for the Van der Pol Map general case for constants a) $\mu = 0$ and $h = 0.1$, (b) $\mu = 0$ and $h = 0.0001$. In all cases $d = 1$.

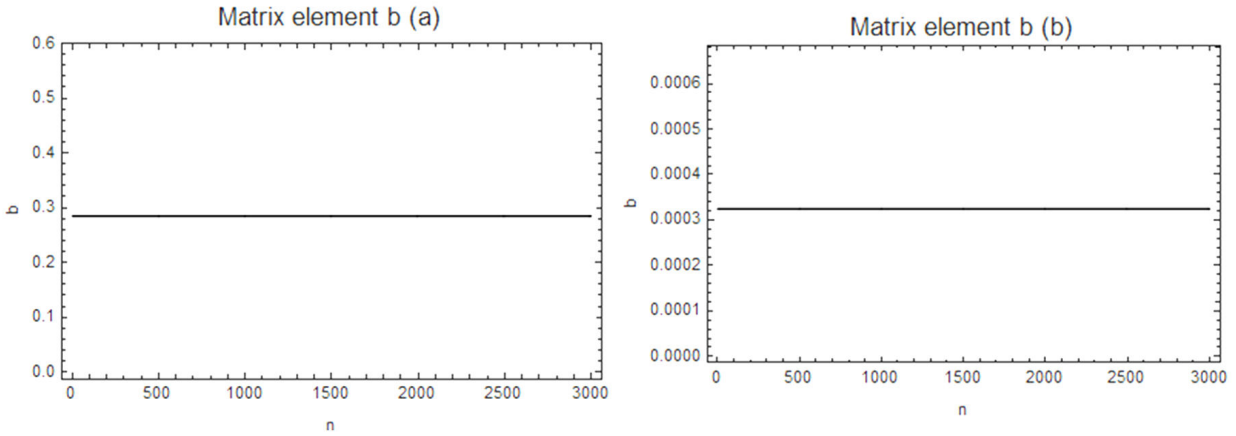

FIGURE 5. Computer calculation of the magnitude of matrix element b_n of the Van der Pol Map generating device for a resonator with $d = 1$ and Van der Pol parameters a) $\mu = 0$ and $h = 0.1$, (b) $\mu = 0$ and $h = 0.0001$, for 3000 round trips.

the phase diagrams (Figs. 2 and 4). Value h was varied for positive numbers till zero, while μ was taken within a range of $-1.5 < \mu < 1.5$. For the $1 < h < 0$ range, there are stable trajectories, and the values of b_n are positive and within the limit of the mirror distance. In the figures below, the values of μ and h are not unique, and there are other allowed combinations. Figure 2 shows the phase-space plots corresponding to different values of parameters μ and h. For example, for parameters $\mu = -1.5$ and $h = 0.0250$, there are no stable states (Fig. 2a)), whereas for $\mu = -0.5$ and $h = 0.1196$, there is a stable fixed point (Fig. 2(b)). In Figs. 2(c-f), we present the cases of the stable limit cycle.

The time series of the matrix element b is presented in Fig. 3. The behavior is quite interesting since different dynamical regimes are observed. The numerical simulations were performed for 2000 iterations for matrix element b of the Van der Pol map generating device for a cavity of unitary length ($d = 1$) and map parameter close to zero. Figures 3(a-c) show damping transients to a stable equilibrium, while Figs. 3(d-f) show others to a stable periodic orbit. One can see from Figs. 3(d-f) how the optical length of the map generating device varies on each round trip in the periodic form (bistability); this would require for a physical implementation such that the physical length of the device, its refractive index, or a combination of both change in time.

The phase diagrams for the general case are shown in Figs. 4 and 5. The process of selection of h and μ was the same as stated above. Valid trajectories were difficult to find in this case due to the matrix complexity; however, as it was found for $\mu = 0$ and h near zero, the trajectories are not stable and increase on each round trip. Notwithstanding the behavior observed in Figs. 5a) and 5b) for matrix element b, after a few iterations, the device's optical thickness remains constant, which should make it easier to achieve a physical implementation of this device. Note that in Fig. 5b), the thickness is near zero, while in Fig. 5a), the thickness is around 0.3.

5. Conclusions

In this paper, a matrix transformation over the Van der Pol map has been proposed to obtain an intracavity element that can yield the same rich, dynamical behavior within a ring phase-conjugated ring cavity. We began our study by ob-

taining the Van der Pol map through the use of the Euler method for discretization; then, we introduced the paraxial matrix analysis (or ABCD propagation law), which was done in order to simplify the analysis, enabling us to express this system as a simple dynamical matrix Equation (3.1). The so-called "Van der Pol beams" (beams that are produced within an optical cavity undergoing Van der Pol map dynamics) were obtained, and they were studied assuming a negligible thickness of the intracavity element, as well as the general case. Numerical calculations were carried out to obtain, within the parameter space, combinations of parameters that yield stable trajectories; this is not an easy task, as the stability of the trajectories is also dependent on the initial value (y_n), and therefore, the trajectories often do not have physical meaning. It is important to remark that we analyzed valid intervals of the system parameters (μ, h, and d).

The range of the μ parameter was selected based on the meaning of the Van der Pol equation, which determines the non-linearity term. However, if one takes values of μ greater than 1.5 or lower than -1.5 for any values of h, the trajectories, and the intracavity element have no physical meaning. Then, for values of μ within this range, we took different values for h and obtained different results with no physical meaning, except for those varying within the $1 < h < 0$ range.

In a simple case of "Van der Pol Beams", we have found trajectories which began in one value and finished around another (refer to Figs. 2a) and 2b)); these types of trajectories allow the intracavity element b_n to reach one value to be stable (refer to Figs. 3a) and 3b)). However, we have also found stable trajectories (Figs. 2d), 2e) and 2f)), which translates into bistability of the intracavity element, and the optical length of the map generating device varies on each round trip in a periodic form; see Figs. 3d), 3e) and 3f). In Fig. 2(c), the trajectory is completely stable, and the parameter of the nonlinearity term is zero; this allows the element b_n to remain constant along with the iterations, which allows for easy implementation of the device.

Next, we moved on to the general case, where the thickness of the intracavity element is greater than zero. Even though the trajectory is not stable because of the increasing values of (y_n, θ_n) (See Fig. 4), the element b_n reaches one value (See Fig. 5), making it possible for the optical length to be constant on each round trip.

Based on the behavior observed, we conclude that the matrix transformation used was successful in generating a dynamic system that preserves the main structures found in the Van der Pol map. The practical implementation of an intracavity element is a complex technical challenge far beyond the aim of this work.

Acknowledgments

The authors acknowledge the professional English proofreading service provided by Mr. Mario Ruiz Berganza.

1. B. Van der Pol and J. Van der Mark, Frequency demultiplication, *Nature*, **120** (1927) 363. https://doi.org/10.1038/120363a0
2. R. FitzHugh, Impulses and physiological states in theoretical models of nerve membranes. *Biophysics J.* **1** (1961) 445. doi: 10.1016/s0006-3495(61)86902-6.
3. J. Nagumo, S. Arimoto, and S. Yoshizawa, An active pulse transmission line simulating nerve axon. *Proc. IRE,* **50** (1962) 2061. doi: 10.1109/JRPROC.1962.288235.
4. J. Cartwright, V. Eguiluz, E. Hernandez-Garcia, and O. Piro, Dynamics of elastic excitable media. *Internat. J. Bifur. Chaos Appl. Sci. Engrg.*, **9** (1999) 2197. https://doi.org/10.1142/S0218127499001620
5. Y. Shuto, Cavity Formation Modeling of Fiber Fuse in Single-Mode Optical Fibers, *Advances in OptoElectronics*, (2017), Volume **2017**, Article ID 5728186, https://doi.org/10.1155/2017/5728186
6. A.D. Case, P.J. Soan, M.J. Damzen and M.H.R. Hutchinson, Coaxial flash-lamp-pumped dye laser with a stimulated Brillouin scattering reflecto. *J.Opt. Soc. Am. B* **9** (1992), 374. https://doi.org/10.1364/JOSAB.9.000374
7. H.-J. Eichler, R. Menzel, and D. Schumann, *Appl. Opt.*, **31** (1992), 5038-5043. https://doi.org/10.1364/OL.16.000569
8. M. O'Connor, V. Devrelis, and J. Munch, in *Proc. Int. Conf. on Lasers'* **95** (1995) 500.
9. M.J. Damzen, V.I. Vlad, V. Babin, and A. Mocofanescu, Stimulated Brillouin Scattering: Fundamentals and Applications, *Institute of Physics, Bristol* (2003). ISBN 9781420033465
10. V. Aboites, Dynamic of a Laser Resonator, *IJPAM* **36** (2007) 352. ISSN 1314-3395
11. M. Wilson, V. Aboites, Optical resonators and dynamic maps, *Proceedings SPIE-The International Society for Optical Engineering*. **8011** (2011) 215. https://doi.org/10.1117/12.903264
12. M. Wilson, V. Aboites, Y. Barmenkov, A. Kir'yanov, *Optical Devices in Communication and Computation*, Chapter XX, Optical Resonators and Dynamic Maps. Ed. Intech, (2012). 17-36. DOI: 10.5772/2859
13. V. Aboites, Y. Barmenkov, A.V. Kiryanov, M. Wilson, Bidimensional dynamic maps in Optical Resonators, *Rev. Mex. Fis*. **60** (2014) 13. ISSN 1870-3542
14. V. Aboites, M. Huicochea, Hénon Beams. *International Journal of Pure and Applied Mathematics.* **65** (2010) 129. ISSN 1314.
15. V. Aboites, D. Liceaga, R. Jaimes-Reategui, J. Garcia, Bogdanov Map for Modelling a Phase-Conjugated Ring Resonator. *Entropy.* **21** (2019) 384. https://doi.org/10.3390/e21040384

16. V. Aboites, D. Liceaga, A. Kir'yanov, M. Wilson, Ikeda Map and Phase Conjugated Ring Resonator Chaotic Dynamics. *Applied Mathematics Information Sciences*. **10** (2016) 1. doi: 10.18576/amis/100608

17. D. Dignowity, M. Wilson, P. Rangel-Fonseca, V. Aboites, Duffing spatial dynamics induced in a double phase-conjugated resonator. *Laser Physics*. **23** (2013) 5002. DOI: 10.1088/1054-660X/23/7/075002

18. V. Aboites, A. Pisarchik, A. Kir'yanov, X. Gomez-Mont, Dynamic Maps in PhaseConjugated Optical Resonators. *Optics Communications*. **283** (2010) 3328. https://doi.org/10.1016/j.optcom.2010.04.063

19. V. Aboites, M. Wilson, F. Lomeli, Standard Map Spatial Dynamics in a Ring-PhaseConjugated Resonator. *Applied Mathematics Information Sciences.* **1** (2015), 1. DOI: 10.12785/amis/paper

20. V. Aboites, Y. Barmenkov, A. Kir'yanov, M. Wilson, Tinkerbell beams in a non-linear ringresonator. *Results in Physics*. **2** (2012) 216. doi.org/10.1016/j.rinp.2012.11.001

21. V. Aboites, M. Wilson, Tinkerbell chaos in a ring phase-conjugated resonator. *Int. J. Pure Appl. Math*. **54** (2009) 429. ISSN 1314-3395

22. Azarkhalili, Behrooz Moghadas, Peyman Rasouli, Mohammad, *Approximation Behavior of Van der Pol Equation: Large and Small Nonlinearity Parameter.* Proceeding of the International MultiConference of Engineers and Computer Scientists 2011, **Vol. II**. ISBN Vol II (pp767-1580): 978-988-19251-2-1

23. Nguyen-Van, Triet and N. Hori, A new discrete-time model for a van del Pol Oscillator. *Proceedings of the SICE Annual Conference*. **10** (2010) 2699. ISBN 978-1-4244-7642-8

24. Y Hafeez, Hafeez. Analytical Study of the Van der Pol Equation in the Autonomous Regime. *Progress in Physics*. **11** (2015) 252.

25. Hallbach, K. Matrix. Representation of Gaussian Optics. *Am. J. Phys.* **32** (1964) 90. https://doi.org/10.1119/1.1970159

26. Wikipedia List of chaotic maps. https://en.wikipedia.org/wiki/Listofchaoticmaps

27. W. Albarakati, N. Lloyd, J. Pearson, Transformation to Lienard form. *Electronic J. Diff. Eqs.* **2000** (2000) 1. ISSN 1072-6691

28. T. Hará, T. Yoneyama, J. Sugie, A necessary and sufficient condition for oscillation of the generalized Lienard equation. *Annali di Matematica pura ed applicata* **154** (1989) 223. ISSN 0373-3114 https://doi.org/10.1007/BF01790349

29. A.O. Ignat'ev, Estimate for the amplitude of the limit cycle of the Lienard equation. *Diff Equat* **53** (2017) 302. https://doi.org/10.1134/S0012266117030028

30. K. Nipp, D. Stoffer, Invariant curves for the discretised van der Pol equation. *Bit Numer Math* **57** (2017) 463. https://doi.org/10.1007/s10543-016-0638-5